

**THE EFFECT OF SURFACE TREATMENT ON THE VOID CALCULATION  
OF THERMOSET COMPOSITE BY USING IMAGE ANALYSIS**

**AHMAD ZULHILMI BIN AHAMAD PAUZI**

**UNIVERSITI TEKNIKAL MALAYSIA MELAKA**

**THE EFFECT OF SURFACE TREATMENT ON THE VOID  
CALCULATION OF THERMOSET COMPOSITE BY USING IMAGE  
ANALYSIS**

**AHMAD ZULHILMI BIN AHAMAD PAUZI**

**This report is submitted  
in fulfillment of the requirement for the degree of  
Bachelor of Mechanical Engineering**


**Faculty of Mechanical Technology and Engineering**

**UNIVERSITI TEKNIKAL MALAYSIA MELAKA**

**JANUARY 2024**

## DECLARATION

I declare that this project report entitled “The Effect of Surface Treatment on The Void Calculation of Thermoset Composite by using Image Analysis” is the result of my own work except as cited in the references


Signature :  .....

Name : AHMAD ZULHILMI BIN AHAMAD PAUZI

Date : 30 JANUARY 2024

## APPROVAL

I hereby declare that I have read this project report and in my opinion this report is sufficient in terms of scope and quality for the award of the degree of Bachelor of Mechanical Engineering.

Signature :  .....

Name of Supervisor : DR. MIZAH BINTI RAMLI

Date : 30 JANUARY 2024

## **DEDICATION**

I dedicate this thesis to the unwavering support and encouragement of my family, whose love has been my anchor throughout this academic journey. To my parents, whose sacrifices and belief in my abilities have fuelled my determination. To my siblings, for their understanding and companionship during the challenging times. I extend my deepest gratitude to my supervisor, whose guidance and expertise have shaped this work. Your invaluable insights and patient mentorship have been instrumental in my academic growth.

This thesis is dedicated to my friends, whose friendship has provided moments of respite and joy amidst the academic rigor. Your friendship has made this journey memorable and enjoyable.

## ABSTRACT

Carbon Fibre-Reinforced Polymer (CFRP) with thermosetting composite with its resin is commonly used in major industries such as high performance automotive and aircraft. Due to unavoidable manufacturing defects which is void formation, the degradation of CFRP performance is occurred. The void formation can be analyzed using image analysis along with its length of specimen. The metallographic grinding and ion polishing are used to obtain surface finishing before undergo microscopic imaging and image analysis. The raw material is divided into 3 regions. In result, the second region consist of highest average void content which is 0.337% of surface's area. Due to high void content at second region, the mechanical properties are degraded. The void content is compared to maximum tensile stress and maximum flexural stress obtained from the mechanical testing. The patent of void content and mechanical properties can be concluded as negative correlation where the increment of void content reduce the mechanical properties.

## ABSTRAK

*Carbon Fibre-Reinforced Polymer (CFRP) dengan komposit termoset sebagai resin biasanya digunakan dalam industri utama seperti automotif berprestasi tinggi dan pesawat kapal terbang. Disebabkan oleh ketidaksempurnaan dalam proses pembuatan yang tidak dapat dielakkan seperti pembentukan rongga udara, prestasi mekanikal CFRP mengalami penurunan. Pembentukan rongga udara dapat dianalisis menggunakan analisis imej terhadap spesimen. Metallographic Grinding dan Ion Polishing digunakan untuk memperoleh permukaan yang rata sebelum menjalani imej mikroskopik dan analisis imej. Bahan mentah ini dibahagikan kepada 3 kawasan. Sebagai hasilnya, kawasan kedua mengandungi kandungan rongga udara purata tertinggi iaitu 0.337% dari kawasan permukaan. Oleh kerana kandungan rongga udara yang tinggi di kawasan kedua, sifat mekanikal terjejas. Kandungan rongga dibandingkan dengan tegangan regangan maksimum dan tegangan lentur maksimum yang diperolehi dari ujian mekanikal. Pateren kandungan rongga udara dan sifat mekanikal dapat disimpulkan sebagai korelasi negatif di mana peningkatan kandungan rongga udara mengurangkan sifat mekanikal.*

## **ACKNOWLEDGEMENT**

I would like to express my deepest gratitude to everyone who has contributed to the completion of this thesis.

First and foremost, I am profoundly thankful to my supervisor, Dr. Mizah Binti Ramli, for their invaluable guidance, unwavering support, and scholarly insights throughout the entire research process. Their expertise and encouragement have been instrumental in shaping the direction of this thesis.

I am indebted to the staff and resources at Universiti Teknikal Malaysia Melaka, without which the execution of this research would not have been possible. The facilities, libraries, and research support services have been crucial to the success of this thesis.

My heartfelt thanks go to my family for their unwavering support and encouragement. Their love and understanding have provided me with the strength and motivation to persevere through the challenges of academic pursuits.

Lastly, I am grateful to my friends who have been a source of inspiration and motivation throughout this academic journey.



## TABLE OF CONTENTS

<b>DECLARATION</b>	<b>ii</b>
<b>APPROVAL</b>	<b>iii</b>
<b>DEDICATION</b>	<b>iv</b>
<b>ABSTRACT</b>	<b>v</b>
<b>ABSTRAK</b>	<b>vi</b>
<b>ACKNOWLEDGEMENT</b>	<b>vii</b>
<b>TABLE OF CONTENTS</b>	<b>viii</b>
<b>LIST OF TABLES</b>	<b>x</b>
<b>LIST OF FIGURES</b>	<b>xi</b>
<b>LIST OF ABBEREVATIONS</b>	<b>xii</b>
<b>LIST OF APPENDICES</b>	<b>xiii</b>
<b>CHAPTER 1 INTRODUCTION</b>	<b>1</b>
1.1 Background	1
1.2 Problem Statement	1
1.3 Objective	3
1.4 Scope of Project	3
<b>CHAPTER 2 LITERATURE REVIEW</b>	<b>4</b>
2.1 Carbon Fibre Reinforced Polymer (CFRP)	4
2.2 Mechanical Properties of Thermoset Composite	8
2.3 Surface Treatment on Surface of Thermoset Composite	9
2.3.1 Metallographic Grinding	9
2.3.2 Ion Polishing	11
2.4 Void Formation on Thermoset Composite	13
2.5 Void Characterization	15
<b>CHAPTER 3 METHODOLOGY</b>	<b>18</b>
3.1 Introduction	18
3.2 Material Preparation	20
3.3 Surface Treatment	21
3.3.1 Metallographic Grinding	21
3.3.2 Ion Polishing	22
3.4 Microscopic Imaging	23

3.5	Void Characterization	25
3.6	Experimental Testing	26
3.6.1	Tensile Test	26
3.6.2	Bending Test	28
<b>CHAPTER 4 RESULTS AND DISCUSSION</b>		<b>31</b>
4.1	Image Analysis based on Surface Treatment	31
4.1.1	Metallographic Grinding	31
4.1.2	Ion Polishing	32
4.2	Void Calculation	34
4.3	Mechanical Properties	37
4.3.1	Tensile Stress	37
4.3.2	Flexural Stress	38
<b>CHAPTER 5 CONCLUSION AND RECOMMENDATIONS</b>		<b>41</b>
5.1	Conclusion	41
5.2	Recommendation for Future Work	42
<b>REFERENCES</b>		<b>43</b>
<b>APPENDIX A</b>		<b>45</b>
<b>APPENDIX B</b>		<b>46</b>
<b>APPENDIX C</b>		<b>47</b>

## LIST OF TABLES

Table 4.1: Void percentage with depth of grinding for each region.	34
Table 4.2: Average void percentage per area for each region.	35
Table 4.3: Experimental result for tensile testing.	37
Table 4.4: Experimental result for flexural testing.	39

## LIST OF FIGURES

Figure 2.1: Concept of carbon fibre reinforced polymer (CFRP).	5
Figure 2.2: (a) Unidirectional and (b) plain weave arrangement of carbon fibre.	6
Figure 2.3: The working principle of ion beam polishing.	12
Figure 2.4: Void formation under microscopic view	14
Figure 3.1: Flowchart of methodology.	19
Figure 3.2: Cutting plan.	20
Figure 3.3: Mounted specimens for grinding process.	21
Figure 3.4: Captured image under microscopic.	24
Figure 3.5: Captured image after void characterization using Fiji ImageJ.	26
Figure 3.6: Rectangular specimens for tensile test.	27
Figure 3.7: Setup of tensile test using UTM.	27
Figure 3.8: Setup of bending test using UTM.	29
Figure 4.1: Surface of Region 2 after 0mm depth of grinding.	31
Figure 4.2: Surface of Region 2 after using ImageJ.	32
Figure 4.3: Side view from observation surface after ion polishing.	32
Figure 4.4: Observation surface after ion polishing.	33
Figure 4.5: Bar chart of void percentage with depth of grinding for each region.	35
Figure 4.6: Bar graph of average void percentage per area against 3 regions.	36
Figure 4.7: Graph of maximum tensile stress against average void.	38
Figure 4.8: Graph of maximum flexural stress against average void.	40

## LIST OF ABBEREVATIONS

CFRP	Carbon Fibre Reinforced Polymer
UD	Unidirectional
PW	Plain Weave
ASTM	American Society for Testing and Materials
FIB	Focused Ion Beam
FBG	Fibre Bragg Grantings
CT	X-ray Computed Tomography
UTM	Universal Testing Machine

## LIST OF APPENDICES

APPENDIX A	Detailed Cutting Plan for Specimens	45
APPENDIX B	Experimental Data for Tensile	46
APPENDIX C	Experimental Data for Bending	47

# CHAPTER 1

## INTRODUCTION

### 1.1 Background

The thermoset composite usually used as polymer in carbon fibre reinforced polymer (CFRP). Along with advance technology in manufacturing of CFRP, defects have always become a topic that may lead to the degradation of CFRP performance. The most significant defect is void formation inside the CFRP where the air is trapped once the CFRP is cured. In this study, the void formation is studied by examining the surface of CFRP under microscopic and analysed using the software Fiji ImageJ to calculate the void percentage. The void formation may vary according to the arrangement of carbon fibre in the CFRP.

The CFRP undergoes a set of experimental testing which are flexural test and tensile test. The data collected from the experimental testing is related to the void percentage.

### 1.2 Problem Statement

The performance and reliability of thermosetting composite materials are significantly impacted by the critical problem of void formation. During the manufacturing process, voids, or trapped air pockets, can develop and affect the composites' mechanical characteristics, structural soundness, and long-term durability. A material's load-bearing capacity, stiffness, and resistance to impact or fatigue are all

decreased when voids are present. Voids or regions unfilled with polymer and fibres are one of the most significant defects which may affect its mechanical properties (Mehdikhani *et al.*, 2019).

The formation and evolution of voids during the processing of fibre-reinforced composites are not the same for all manufacturing techniques due to the difference in thermodynamics and rheological phenomena happening in these processes (Mehdikhani *et al.*, 2019). The use of thermosetting composites in various industries must be advanced by understanding the factors leading to void formation and creating efficient ways to mitigate or minimize voids. Understanding the mechanisms that cause void formation, figuring out the underlying causes, and coming up with ways to measure and regulate the void content within the composite structure are the problems. The main sources of voids are air entrapment either during impregnation or during laying up, which causes intra-laminar void defects and inter-laminar void defects (Fu & Yao, 2022).

In thermosetting composites, void formation is caused by a number of factors. A localized area with insufficient resin can cause voids if the reinforcing fibres are not sufficiently impregnated during the resin infusion process. During the fabrication process, ineffective air bubble removal, poor fibre wetting, and improper fibre alignment can all lead to void formation. Additionally, voids can develop within the material as a result of chemical reactions, such as the release of volatile compounds during curing.

Understanding the underlying mechanisms deeply and creating practical methods for void reduction or elimination are essential to solving the issue of void formation in thermosetting composites. This entails looking into how process variables



like resin infusion methods, curing environments, and post-cure treatments affect the formation of voids. To accurately measure and assess the void content within the composite structure, advanced characterization techniques, such as image analysis and non-destructive testing methods, are also required.

### **1.3 Objective**

The objectives of this project are as follows:

1. To study the effect of surface preparation by using metallographic grinding and ion polishing.
2. To analyse the void percentage at different depths of grinding and polishing.
3. To analyse the relation between mechanical properties with void percentage.

### **1.4 Scope of Project**

The scopes of this project are:

1. The surface treatment techniques used are metallographic grinding and ion polishing.
2. The material used for the study is carbon fibres with thermosetting composite.
3. The void characterization and percentage are quantified using Fiji ImageJ analysis.
4. The mechanical properties of the thermosetting composite are tested by applying the experiment of tensile and flexural tests.

## **CHAPTER 2**

### **LITERATURE REVIEW**

#### **2.1 Carbon Fibre Reinforced Polymer (CFRP)**

The composite material known as carbon fibre reinforced polymer (CFRP) is a combination of carbon fibres and a polymer matrix. Carbon fibres offer superior strength and stiffness, whereas the polymer matrix serves to bind the fibres and facilitate load transfer between them. Carbon fibre reinforced polymer (CFRP) is widely recognized for its exceptional strength-to-mass ratio, rendering it a highly popular material in various sectors such as aerospace, automotive, and other weight-sensitive industries. The material is recognized for its ability to resist corrosion, exhibit durability, and withstand fatigue. Carbon fibre reinforced polymer (CFRP) can be produced through diverse techniques such as manual layup, filament winding, and resin transfer molding. Figure 2.1 shows concept of carbon fibre reinforced polymer.

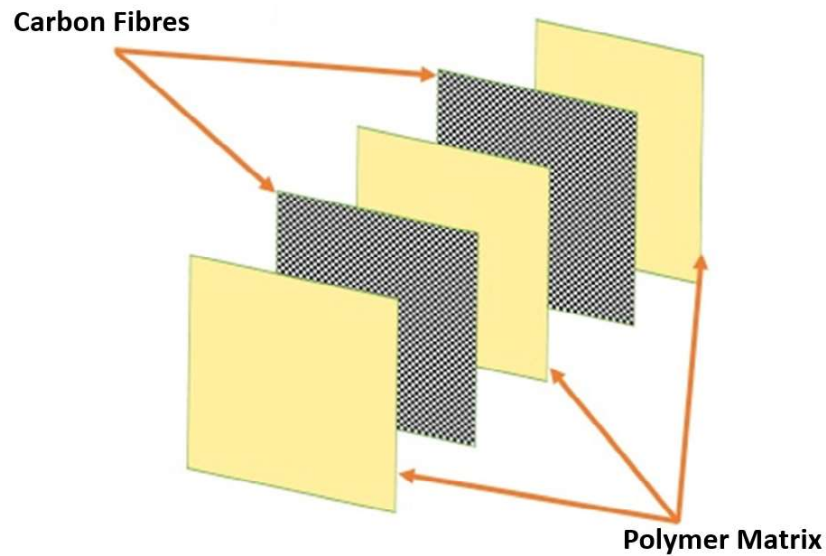


Figure 2.1: Concept of carbon fibre reinforced polymer (CFRP).

The utilization of carbon filler is a common technique in the reinforcement of fibre materials, aimed at enhancing their mechanical and thermal characteristics. This filler type is classified as inorganic. Commonly, it is incorporated into the matrix material, such as a resin, with the aim of enhancing the rigidity, durability, and thermal resistance of the resultant composite material (Hall *et al.*, 2022). Carbon fillers, such as carbon fibres, carbon nanotubes, and graphene, are recognized for their exceptional strength-to-weight ratio, low thermal expansion, and superior electrical conductivity. The incorporation of fibre reinforcement, particularly carbon fibre, into a composite material can lead to enhanced mechanical and thermal characteristics, thereby expanding its potential utilization in various sectors including aerospace, automotive, and construction.

Unidirectional (UD) carbon fabrics are characterized by the alignment of all their fibres in a single direction, whereas Plain Weave (PW) carbon fabrics exhibit a criss-cross pattern in which fibres are woven over and under each other (Helmus *et al.*, 2017). Unidirectional (UD) fabrics exhibit superior strength along the orientation of

their fibres, whereas Plain Weave (PW) fabrics demonstrate more consistent strength across all orientations (Hall *et al.*, 2022). The article's context explains that the UD composites exhibited reduced densities in comparison to the PW composites, which can be attributed to variations in compaction during the fabrication procedure (Hall *et al.*, 2022). Figure 2.2 shows the unidirectional and plain weave arrangement of carbon fibre.

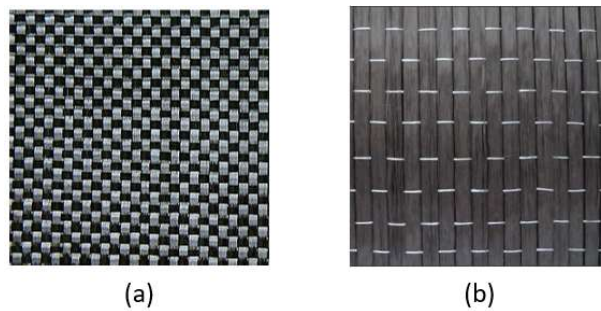


Figure 2.2: (a) Unidirectional and (b) plain weave arrangement of carbon fibre.

Thermosets represent a category of polymers that undergo curing or crosslinking in the course of processing, leading to the formation of a three-dimensional network configuration that is impervious to melting or reshaping after solidification. These materials find extensive usage across diverse applications such as adhesives, coatings, and composites (U, Remanan and Jayanarayanan, 2020).

There are three common types of resin of thermoset composite used. Epoxy resin is a frequently encountered thermoset that finds extensive employment in aerospace and other high-performance composites. Epoxy resins exhibit exceptional mechanical characteristics, such as elevated strength and rigidity, coupled with commendable resistance to heat and chemical agents. Nevertheless, ceramics exhibit a tendency towards fragility and susceptibility to fracture in specific circumstances.

Polyester resin is a variety of thermoset that is frequently employed in marine and automotive composites. Polyester resins exhibit favourable mechanical characteristics and are comparatively cost-effective. However, they are susceptible to shrinkage and may present challenges during handling and processing.

Phenolic resins are a prevalent category of thermosetting polymers that find extensive usage in various industrial applications, including but not limited to adhesives and coatings. The material in question exhibits exceptional thermal and chemical resistance, in addition to possessing favourable electrical insulating characteristics. Nevertheless, ceramics exhibit a tendency to fracture easily, and their processing can pose challenges.

In general, CFRPs represent a highly promising class of materials that exhibit exceptional strength-to-weight ratios, superior fatigue resistance, and commendable thermal stability. These have been extensively utilized across diverse sectors such as aerospace, automotive, and sports equipment. The manipulation of fibre orientation, fibre volume fraction, and matrix properties can enable customization of the mechanical characteristics of CFRPs. Nevertheless, the production procedure of CFRPs is intricate and costly, thereby constraining their extensive acceptance. However, current efforts in research and development are concentrated on enhancing the production methodology and diminishing the expenses associated with Carbon Fibre Reinforced Polymers (CFRPs)(Hall *et al.*, 2022). Due to ongoing technological progress, carbon fibre reinforced polymers (CFRPs) possess the capability to replace conventional materials across various domains, resulting in the development of structures that are more lightweight, robust, and effective.

## 2.2 Mechanical Properties of Thermoset Composite

The outstanding mechanical characteristics of carbon fibre reinforced polymer (CFRP) composites make them a subject of considerable interest in recent years. The mechanical characteristics of carbon fibre reinforced polymer (CFRP) composites are primarily impacted by the properties of the constituent materials, including the carbon fibres and polymer matrix, in addition to the manufacturing methodology employed to fabricate the composite(Baran *et al.*, 2017).

The carbon fibres utilized in CFRP composites are renowned for their exceptional strength and stiffness, rendering them well-suited for deployment in structural contexts. Polyacrylonitrile (PAN) or pitch are commonly utilized materials for the production of fibres. These fibres are distinguished by their tensile strength, modulus of elasticity, and strain-to-failure. The range of tensile strength exhibited by carbon fibres spans from 1.5 to 7 GPa, with a corresponding range of modulus of elasticity from 100 to 700 GPa (Baran *et al.*, 2017). The ultimate tensile strength of carbon fibres is generally in the vicinity of 1.

Thermosetting resins, such as epoxy or polyester, are commonly utilized as the polymer matrix in CFRP composites. The incorporation of a polymer matrix into the composite material confers enhanced mechanical strength and durability, in addition to heightened resilience against various environmental stressors, including moisture and ultraviolet radiation(Baran *et al.*, 2017). The mechanical characteristics of the polymer matrix are subject to the influence of various factors, including the curing temperature and duration, as well as the nature and quantity of the curing agent employed.

The mechanical characteristics of carbon fibre reinforced polymer (CFRP) are dependent upon an array of factors, including but not limited to the matrix material

employed, the orientation of the fibres, and the specific manufacturing techniques utilized (Hassan *et al.*, 2022). In comparison to conventional materials such as steel and aluminium, CFRP composites exhibit superior strength-to-weight ratios, stiffness, and fatigue resistance. Additionally, they exhibit exceptional resistance to corrosion and possess high thermal stability. The mechanical properties of CFRP may exhibit significant variability based on the particular application and design specifications.

## **2.3 Surface Treatment on Surface of Thermoset Composite**

### **2.3.1 Metallographic Grinding**

Metallographic grinding is a technique employed to ready metal specimens for microscopic examination. The process entails the abrasion and refinement of the metal surface to eliminate any superficial irregularities or imperfections, such as abrasions, grooves, or fractures, and to expose the material's microstructural composition (Wang *et al.*, 2020). The process of metallographic grinding holds significant importance in the field of materials science and engineering, as it helps the examination of the microscopic characteristics and performance of material. The procedure involves the utilisation of abrasive substances, such as silicon carbide or diamond, to eliminate material from the material's surface (Wang *et al.*, 2020). Afterwards, the material is polished with a sequence of increasingly fine abrasives to get a polished and reflective surface. The process of metallographic grinding is frequently used in the production and examination of solid elements as well as in the exploration and innovation of new substances.

The preparation of a well-crafted specimen for CFRP composites through metallographic grinding involves a number of related procedures. The CFRP specimen is initially analysed with precision to acquire a representative part for analytical purposes. After that, the specimen is attached onto a holder or embedding medium to ensure structural integrity throughout the course of the grinding procedure. Suitable specimen mounting is necessary to ensure safe holding of the specimen and to minimize the possibility of delamination or damage during next grinding procedures.

After being attached, the carbon fibre reinforced polymer specimen goes through to a gradual grinding process utilizing abrasive papers or grinding stones of different grit sizes. The aim is to eliminate superficial layers and get a level and uniform surface that allows precise examination under microscopy or other methods of characterization. It is essential to exercise strict control over the grinding process to avoid the possibility of excessive heat generation (Abdelal and Donaldson, 2018). This can have negative impacts on the polymer matrix of the composite or lead to thermal degradation of the carbon fibres.

The utilization of metallographic grinding in the examination of reinforced carbon fibre polymer composites presents numerous benefits for material analysis. The initial advantage of this technique is its ability to create specimens with well-defined surface properties, allowing the precise analysis and evaluation of the composite's microstructural features (Wang *et al.*, 2020). The process helps in the removal of surface irregularities, such as voids, regions with excessive resin content, or fibre detachment, all of which may have an impact on the mechanical characteristics of the composite. Metallographic grinding is a technique that enables researchers and engineers to evaluate the carbon fibre distribution, alignment, and integrity within the



polymer matrix. This assessment provides significant insights into the composite's structural integrity and performance.

To summarize, the process of metallographic grinding is an important method of surface treatment utilized in the preparation and examination of reinforced carbon fibre polymer composites. Through the application of controlled surface finishes and the elimination of surface imperfections, the composite's microstructure can be precisely analysed, which allows for the gathering of significant observations regarding its characteristics, functionality, and structural integrity. The process of metallographic grinding is of utmost importance in the optimization of Carbon Fibre Reinforced Polymer (CFRP) composite materials for various uses, and in contributing to progress in the field of composite technology.

### **2.3.2 Ion Polishing**

Ion polishing is a surface modification methodology that involves the utilisation of ion beams to eliminate material from a surface. The methodology has been widely applied across various fields, that involve optics, electronics, and materials science. The fundamental principles of ion polishing are rooted in the relationship between the ion beam and the material surface as shown in Figure 2.3. The contact of ion beam onto a surface result in sputtering, which is the banishing of atoms from the surface resulting to the ion impact (Xia *et al.*, 2020). The removal of material from a surface can be achieved through the sputtering process, whereby the ion beam energy and angle of incidence can be manipulated by adjusting the voltage to obtain the result.

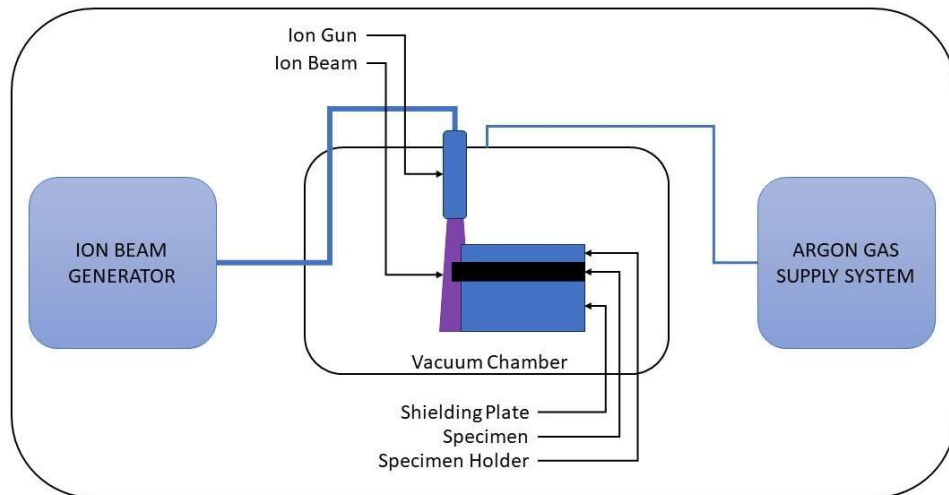


Figure 2.3: The working principle of ion beam polishing.

The utilisation of ion polishing is primarily observed in the production of optical surfaces of outstanding quality. The above-mentioned methodology has been used for the purpose of eliminating unimportant imperfections and enhancing the surface texture of optical components, including but not limited to mirrors, lenses, and prisms. Ion polishing is a technique that finds its application in the electronics sector for the purpose of preparing specimens intended for microscopy and analysis. This methodology has the capability of removing superficial imperfections and impairments that may arise from mechanical polishing or other comparable surface preparation methodologies.

The most recent developments in ion polishing have been directed towards enhancing the accuracy and effectiveness of the method. A useful methodology involves the utilisation of focused ion beams (FIBs) for the purpose of targeted removal of material from different areas of a given specimen. Fibre Bragg Gratings (FBGs) possess the capability to generate intricate designs and architectures on a given surface with exceptional accuracy (Xia *et al.*, 2020). An additional advancement in the field involves the integration of ion polishing with other methodologies for surface

preparation, including chemical etching and mechanical polishing. The implementation of hybrid techniques has the potential to enhance the surface finish quality and decrease the duration of surface preparation.

To conclude, ion polishing is a complex surface finishing technique that finds utility in diverse domains. The methodology relies on the relationship between ion beams and the material surface and has the potential to enhance the surface texture and eliminate surface anomalies. Contemporary improvements in the field have prioritised the enhancement of the accuracy and effectiveness of the methodology, as well as the integration of ion polishing with alternative surface preparation methodologies.

#### **2.4 Void Formation on Thermoset Composite**

In composite materials, voids frequently occur, which can negatively interfere with their mechanical characteristics. Numerous investigations have been carried out to look into the reasons for and implications of void development in composite materials. The presence of air or gas pockets during the manufacturing process is one of the main reasons why voids arise (Zhang, Heider and Gillespie, 2017). Void development can happen if these pockets become trapped in between the layers of the composite material. By removing the air or gas pockets, vacuum bagging and autoclave operations can help to decrease the creation of voids. Figure 2.4 shows void formation under microscopic view.

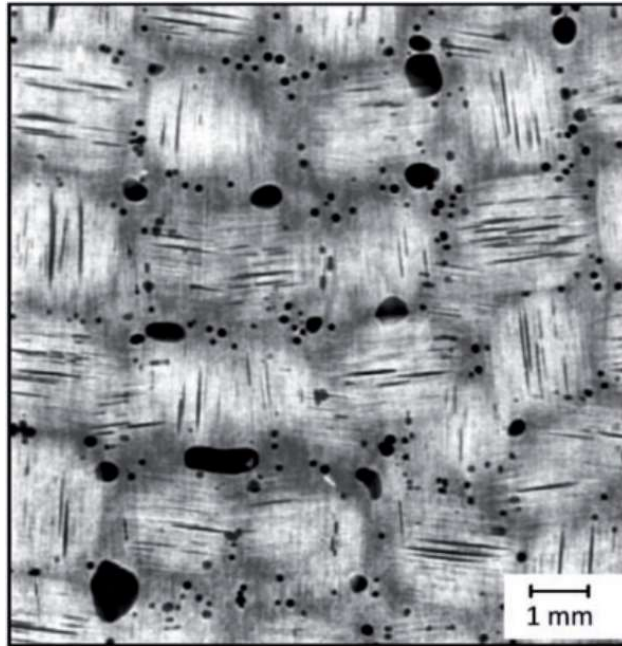


Figure 2.4: Void formation under microscopic view

The curing process is another element that may contribute to the creation of voids. The resin may not fully cure, resulting in the production of voids, if the curing temperature is too low or the curing time is too short (Jiang *et al.*, 2019). On the other side, the resin may over-cure if the curing temperature is too high or the curing period is too long, resulting in the production of fractures and other flaws.

The formation of voids can also be influenced by the kind of reinforcement material employed in the composite. For instance, voids may develop in the composite material if the fibres are not properly aligned or if there are spaces between the fibres (Gao *et al.*, 2020). The mechanical properties of composite materials can be greatly affected by the presence of voids. The material's susceptibility to wear and failure as well as its strength and stiffness can all be affected by voids (Jiang *et al.*, 2019; Saenz-Castillo *et al.*, 2019). Consequently, it's critical to reduce the development of voids during the production process.

For the purpose of locating and measuring voids in composite materials, several approaches have been developed. These consist of micro-CT, X-ray computed tomography (CT), and ultrasonic testing (Mehdikhani *et al.*, 2019). These methods can help identify the sources of void development and create preventative measures by providing useful information about the size, shape, and location of voids in the material.

Overall, void formation is a frequent problem in composite materials that can have a big impact on their mechanical characteristics. Numerous factors, including the manufacturing method, curing procedure, and reinforcement material, might contribute to the creation of voids. Finding the reasons of void generation and formulating preventative measures depend on finding and quantifying voids in composite materials.

## **2.5 Void Characterization**

The characterization of voids provides a major role in the area of composite materials research, due to the considerable impact that voids may have on the mechanical properties of the material. Various methods have been developed for the purpose of characterizing voids in composite materials, such as ultrasonic scanning, serial sectioning, and X-ray computed tomography (CT).

The utilization of ultrasonic scanning as a straightforward methodology offers full information regarding the void content present within the whole of the panel. The methodology involves the transmission of ultrasonic waves across the substance, followed by the computation of the duration taken for the waves to return after reflection (Hudson *et al.*, 2017; Abdelal and Donaldson, 2018). The method has been

employed for the purpose of characterizing voids in composite materials, even its precision is limited by the dimensions and configuration of the voids.

The process of serial sectioning involves breaking down of the specimen into thin parts, followed by an examination of every part through a microscope (Opelt, Cândido and Rezende, 2018). This methodology offers extensive information into the dimensions, configuration, and dispersion of hollows, even being a non-reversible methodology that is applicable just to a restricted set of specimens.

X-ray computed tomography (CT) is a simple imaging technique that offers comprehensive three-dimensional spatial information on voids. This methodology requires the utilization of X-ray scanning and computational algorithms to generate a three-dimensional representation of the material (Na, Kwon and Yu, 2018). X-ray computed tomography (CT) has shown a high degree of precision in void characterization. However, it is a costly method and its availability is limited.

The researchers conducted a void characterization utilizing all three methodologies. The findings indicate that a direct relationship exists between the level of vacuum used during the manufacturing process and the extent of void content observed. Specifically, a decrease in vacuum pressure resulted in a corresponding increase in void content. Furthermore, it was observed that voids were only present in the resin-rich area located between fibre tows or between layers, rather than in the spaces between resin regions within fibre tows. The specimens exposed to higher vacuum conditions showed an increased number of spherical or circular shapes, while the specimens exposed to lower vacuum conditions displayed a rate of cylindrical shapes located between fibre tows. The region nearby to the midplane of the laminate shown a greater quantity of voids, as well as voids of larger dimensions.

To summarize, the characterization of voids holds significant importance in the field of composite materials research, and various methodologies have been devised to effectively analyze voids present in composite materials. Various methodologies have their own set of benefits and drawbacks, and it is relying upon researchers to select the methodology that is most appropriate for their research requirements.

## CHAPTER 3

### METHODOLOGY

#### 3.1 Introduction

This section elaborates on the methodology used in this study to determine the void percentage of the thermoset composite under various arrangements of carbon fibre reinforcement. Figure 3.1 represents the methodology flowchart of the project. The beginning of this project involves understanding the characterization of voids and their formation on the thermoset composite. The characterization of voids can be achieved through microscopic imaging analysis using the Fiji ImageJ software. The data acquired will be related to the configuration of carbon fibres that have been reinforced. The thermoset composite specimens are put through to experimental testing, which includes both bending and tensile tests.



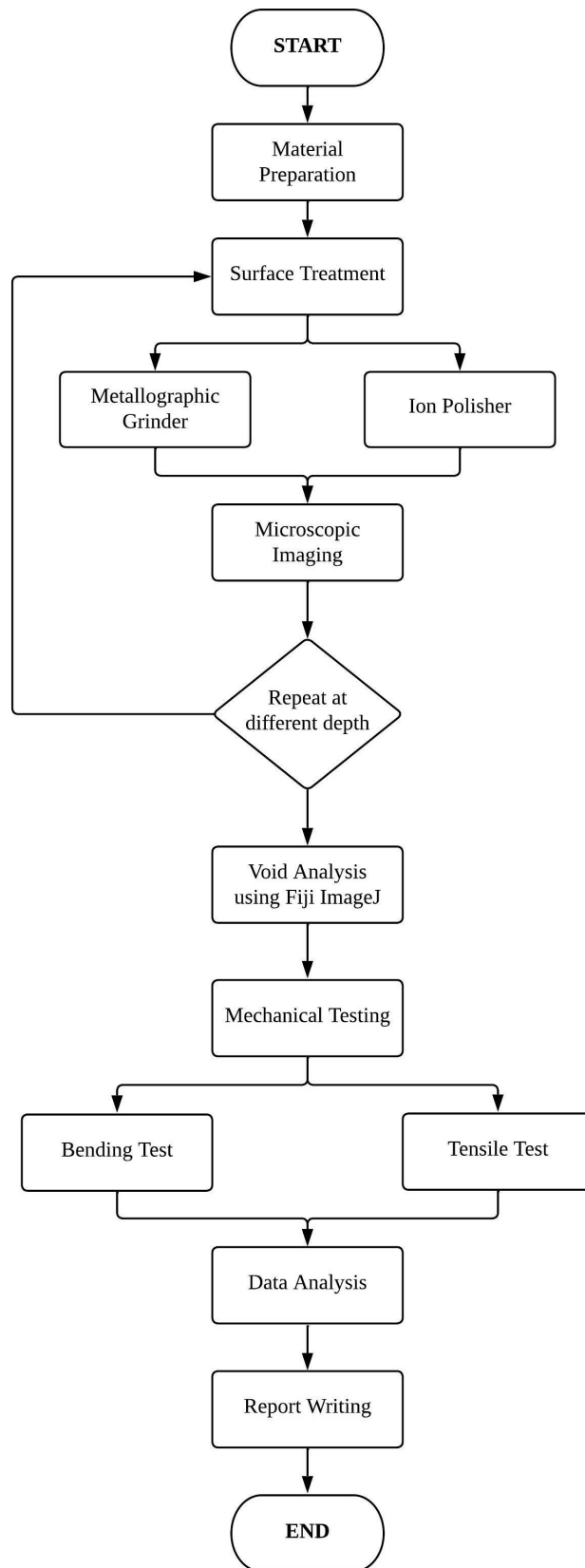


Figure 3.1: Flowchart of methodology.

### 3.2 Material Preparation

In terms of material preparation, one configurations of reinforced carbon fibres was chosen, which is woven. The thermoset composite used had a thickness of 2.6 mm. The materials had been obtained from an industrial sector that specializes in the production of carbon fibre reinforced polymers. From the same plate of raw material, the partition of 3 regions had been made as shown in Figure 3.2. Each region consisted of 1 specimen of ion polishing, 1 specimen of metallographic, 1 specimen for each mechanical testing. In advance of starting surface treatment, the materials is resized into specimens to make it easier to mount for both surface treatment techniques, which are metallographic grinding and ion polishing. On the other hand, the materials mentioned above undergo cutting process into suitable size of specimens for the purpose of experimental testing, specifically in the form of bending and tensile tests. The details of measurement can be referred to Appendix A.

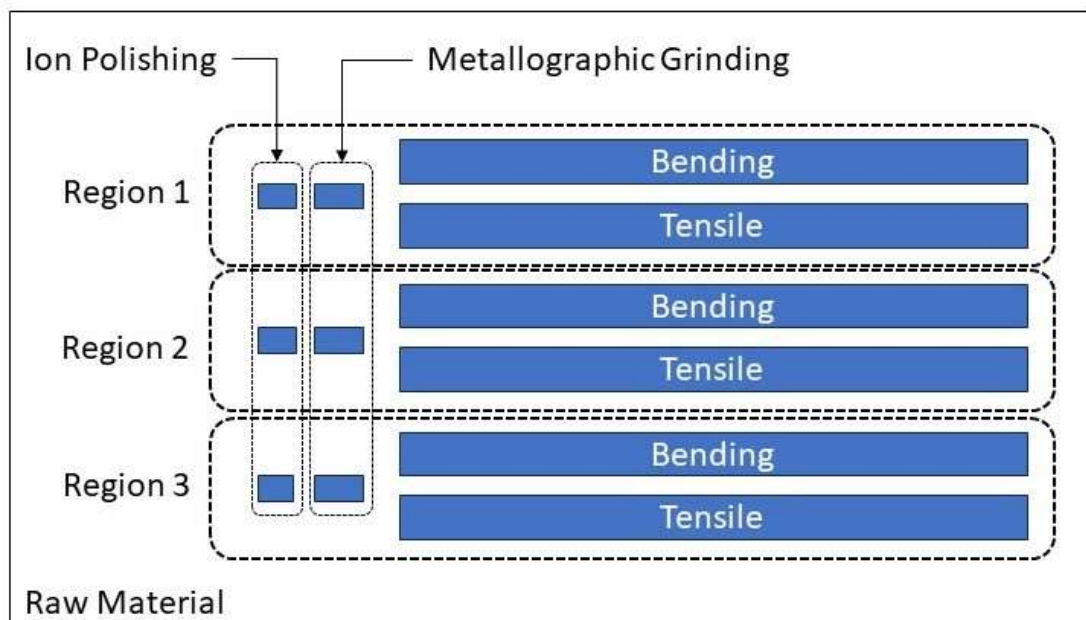


Figure 3.2: Cutting plan.

### 3.3 Surface Treatment

#### 3.3.1 Metallographic Grinding

Metallographic grinding used to remove the material from the specimens' surface. The specimens are mounted to the mounting mold for holding the specimens during grinding process as shown in Figure 3.3. The specimens are put into mounting mold with the resins and hardened.

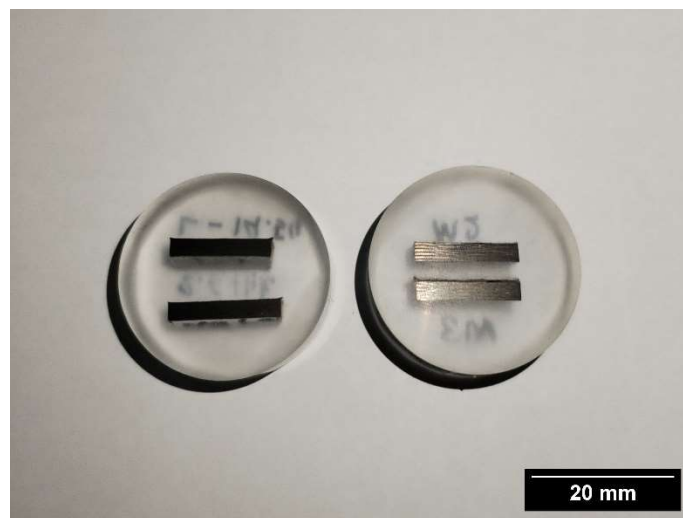


Figure 3.3: Mounted specimens for grinding process.

For the grinding process, the mold of specimens is placed. After mounting the specimen, the initial stage of the grinding process involved applying the technique of coarse grinding. The process of coarse grinding used of abrasive papers known as wheels that possess a lower grit size of 180. The grinding apparatus was fitted with the selected abrasive substance, and a coolant was applied to the specimen externally to prevent overheating and remove debris. The desired surface flatness and roughness can be achieved by gradually removing material through the application of even pressure and back-and-forth movement of the specimen. The process of coarse grinding served to remove surface irregularities and mitigate any prior preparation damage.

After the initial stage of coarse grinding, another stage of fine grinding proceeded. This step involved the use of abrasive papers or wheels with a higher grit size, which is 320. Similar to the process of coarse grinding, the application of coolant and the regulation of pressure were used. The objective of the fine grinding process was to remove the abrasions that are left behind by the initial coarse grinding phase and then improve the surface of the specimen, leading to a polished and clean visual aspect.

Upon completion of the grinding stages, the specimen proceeded to the fine grinding with higher grit size which was 800. The optimisation of grinding parameters, including pressure, speed, and grinding time, is customised to meet the requirements of the specimen and the selected polishing solution. The process of polishing persists until achieving a surface finish that resembles that of a mirror.

### **3.3.2 Ion Polishing**

The preparation of the specimen involved securely placing it to a specimen holder. Making sure the appropriate alignment and stability of the specimen was a crucial aspect of the ion polishing procedure. Furthermore, the surface of the specimen is carefully cleansed to remove any residues or impurities that may interfere with the ion polishing process.

Upon preparation of the specimen, the process of evacuating the vacuum chamber started through the activation of the vacuum pump. The chamber underwent to evacuation until the desired pressure level is achieved. The effectiveness of the ion beam requires the presence of a high vacuum environment.

The ion beam parameters, including beam voltage, polishing time and argon supplied, were modified to suit the specimen material and the desired rate of material removal. To achieve consistent material removal, the specimen surface was subjected to an ion beam that is directed perpendicular to it. The uniformity of material removal throughout the specimen surface was ensured by controlling the ion beam scanning rate and pattern.

The ion polishing procedure was carried out until the intended level of surface quality was attained. Upon completion of the ion polishing process, the ion beam would be deactivated, and the vacuum chamber was vented. Then, the specimen was removed from the holder and treated to a finishing cleaning procedure to eliminate any residual substances that may have developed from the ion milling operation. A suitable solvent is used for cleaning, and the specimen was allowed to dry completely before further analysis.

### **3.4 Microscopic Imaging**

Microscopic imaging techniques involved a sequence of procedures aimed at visualising and recording detailed images of specimens at a microscopic scale. The initial step involved the preparation of the sample, that it was subjected to suitable treatment and mounted for microscopic analysis. The process had involved the placement of the specimen on a slide designed for microscopic observation, and the use of dyeing agents to enhance contrast.

After that, the microscope was set up by fine-tuning the necessary parameters, such as the degree of illumination, focal point, and amplification. Accurate

measurement and image acquisition were dependent upon the precise calibration of the microscope. Afterwards, the sample that had been prepared was placed onto the microscope holder, with appropriate attention to its central positioning and secured attachment. The precise positioning of the sample below the microscope can be achieved through the utilisation of mechanical controls.

The process of acquiring images involved the optimisation of image quality through the adjustment of microscope settings, including focus, brightness, and contrast. The capture of images was achieved through the use of the microscope's integrated camera. The availability of specialised software for image acquisition, control, and analysis may vary depending on the microscope and imaging system in use. The captured images were transferred to a computer for the next processing and analysis. Figure 3.4 shows the image under microscopic view. Image processing software was utilised for the purpose of improving the quality of images, modifying the brightness and contrast, and implementing other requisite alterations. Microscopic images were used to compare, interpretation, and correlate in this study.



Figure 3.4: Captured image under microscopic.

### **3.5 Void Characterization**

The image of specimens under microscopic was inserted into Fiji ImageJ by selecting "File" from the menu and choosing "Open." This allowed the image to be accessed within the software for further processing. To ensure accurate measurements, the "Set Scale" option was selected under the "Image" menu. The known distance and corresponding unit of measurement obtained from the microscopic image are entered. This step allowed Fiji ImageJ to establish a proper scale for subsequent measurements.

To verify the accuracy of the scale, a line was drawn from the left to the right using the line tool. This enabled the confirmation of the correct scale and ensured reliable measurements. Next, the image was converted to 8-bit grayscale by selecting the "Type" option under the "Image" menu and choosing "8-bit" from the available options. This conversion simplified the subsequent image processing steps by reducing the image to grayscale representation.

The threshold was adjusted to identify the void areas in the image. Under the "Adjust" option within the "Image" menu, the threshold sliders are manipulated until the void areas appear as red regions. Once the threshold was set, it was applied to the image by clicking on the "Set" button and selecting "OK." This ensured that the subsequent analysis focused on the identified void areas. The holes within the void regions were filled by selecting the "Fill Holes" option under the "Binary" submenu within the "Process" menu. This step ensured that the entire void areas were accurately accounted for in the analysis, without any missing data.

After that, outlines were created around the void areas to improve visualization. This was achieved by selecting the "Outlines" option under the "Binary" submenu within the "Process" menu. This step made the void regions easily distinguishable for

further analysis and evaluation. To measure the area and area fraction of the void regions, the "Set Measurements" option was chosen under the "Analyze" menu. The options for "Area" and "Area Fraction" were enabled in the measurement settings.

Finally, the measurements were performed on the outlined void areas by selecting the "Measure" option under the "Analyze" menu. Fiji ImageJ calculated the area and area fraction based on the set measurement parameters, providing quantitative results for further analysis and interpretation. By following these procedures in Fiji/ImageJ, the void areas in the image were accurately measured and analysed, facilitating comprehensive and quantitative analysis of the sample under study. Figure 3.5 shows the Figure 3.4 after process of void characterization using Fiji ImageJ.

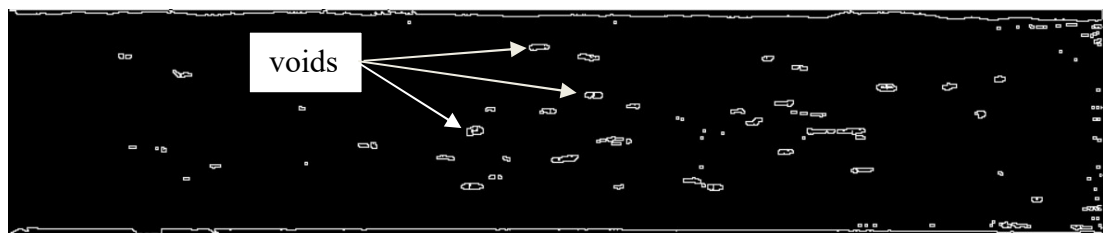


Figure 3.5: Captured image after void characterization using Fiji ImageJ.

## **3.6 Experimental Testing**

### **3.6.1 Tensile Test**

The initial step in conducting the tensile test involved the preparation of samples of the CFRP material. These samples were cut into flat rectangular shape specimens as shown in Figure 3.6, which match to the dimensions and geometry outlined in ASTM D3039. A Universal Testing Machine (UTM) had been set up with suitable grips to conduct tensile testing on CFRP materials. The Universal Testing Machine (UTM) was calibrated according to the manufacturer's guidelines to



guarantee precise force and elongation readings during the testing process. Figure 3.7 shows the setup of tensile test using universal testing machine (UTM).

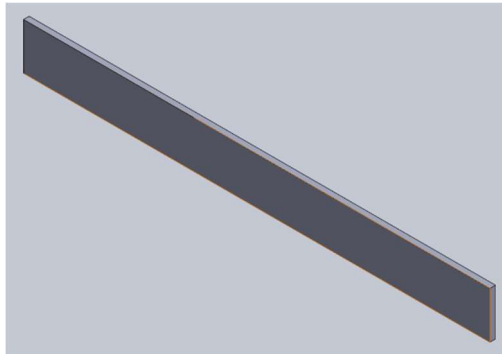


Figure 3.6: Rectangular specimens for tensile test.

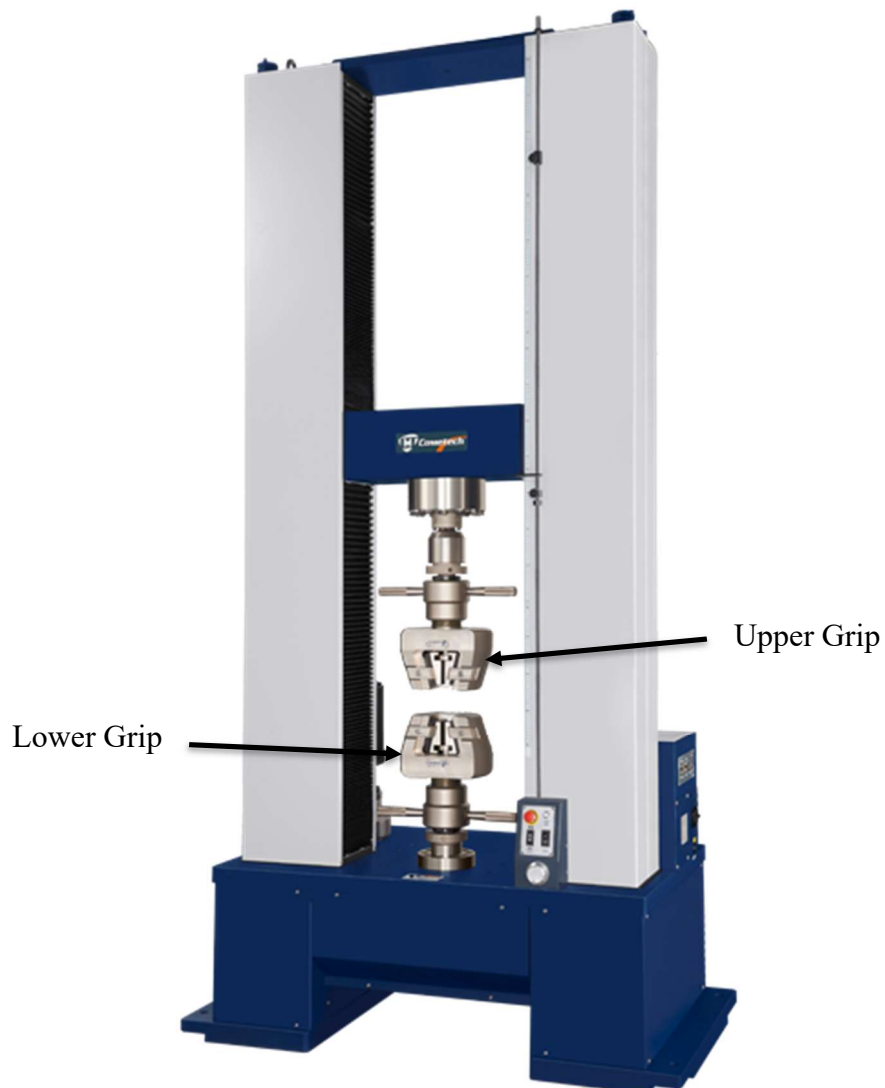


Figure 3.7: Setup of tensile test using UTM.

The upper grip of the Universal Testing Machine (UTM) was used to firmly secure one end of the specimen, whereas the lower grip was employed to fix the other end. Proper alignment of the specimen within the grips and ensuring that the applied load was in line with the axis of the specimen are critical aspects.

The Universal Testing Machine (UTM) was initiated, and a consistent tensile load was exerted on the sample at a uniform movement which was 5mm/min, conforming to the specified testing velocity and strain rate. During the examination, the exerted force and elongation, also known as strain, were consistently recorded and observed at fixed time intervals.

The experiment involved the collection of data related to the applied force (load) and the corresponding elongation (strain) until the specimen reaches failure. The ASTM D3039 guidelines were followed to record the maximum load, yield point elongation, and fracture point.

### **3.6.2 Bending Test**

The bending test is initiated by preparing representative specimens in complying to the dimensions stated by ASTM D7263. A universal testing machine (UTM) was configured with a suitable bending tester and an appropriate fixture to perform a cantilever bending test on a given sample. The calibration of the testing apparatus was performed in accordance with the guidelines provided by the manufacturer to guarantee precise measurements of force and deflection throughout the testing process. Figure 3.8 shows the setup of bending test machine.



Figure 3.8: Setup of bending test using UTM.

The specimens were fixed firmly onto the bending fixture of the testing apparatus, with careful consideration given to their alignment with the reference points of the fixture. It was ensured that the specimens were placed in the way that allows the desired bending direction during every phase of the test. The determination of test parameters, which was bending speed and support distance, was based on the prescribed requirements stated in ASTM D7263. These variables determined the testing conditions and had an impact on the outcome bending properties.

The testing apparatus was activated, and the flexural examination was started. The apparatus gradually and smoothly generated the bending force on the specimen at a predetermined speed which was 5 mm/min, which allows for accurate observation and measurement of the bending characteristics. During the testing process, the bending force applied, and the corresponding deflection and displacement of the specimen were continuously monitored and recorded. The data were gathered periodically according to the established protocol to effectively record the performance of the CFRP during the bending testing.

The testing process continued until the specimen attained the intended endpoint of the test, which could potentially entail a point of failure. The ASTM D7263 guidelines were followed to in order to determine the suitable end point of the flexural examination. The data that had been gathered was subjected to analysis in order to identify the bending characteristics of the CFRP, including the bending force, flexural rigidity, and the correlation between force and deflection.

## CHAPTER 4

### RESULTS AND DISCUSSION

#### 4.1 Image Analysis based on Surface Treatment

The surface treatments consist of two techniques as stated in methodology before. The result of surface treatment is shown in subchapter 4.1.1 and 4.1.2.

##### 4.1.1 Metallographic Grinding

Figure 4.1 below shows the Region 2 after metallographic grinding at depth of 0 mm. The surface of Region 2 is finished with 800 grit size. However, the scratched lines still appear on the surface but due to its tiny size, the scratches barely seen. Before using image analyser which is ImageJ, the void formation can be located by observing darken area of the surface. This observation is very helpful when the image is applied to ImageJ to ensure the void is selected correctly.



Figure 4.1: Surface of Region 2 after 0mm depth of grinding.

The Figure 4.2 below show the Figure 4.2 after applying to ImageJ analyser. The void formation is selected based on threshold applied to the image from microscopic imaging. The void is automatically calculated using “Measure” tool from ImageJ.

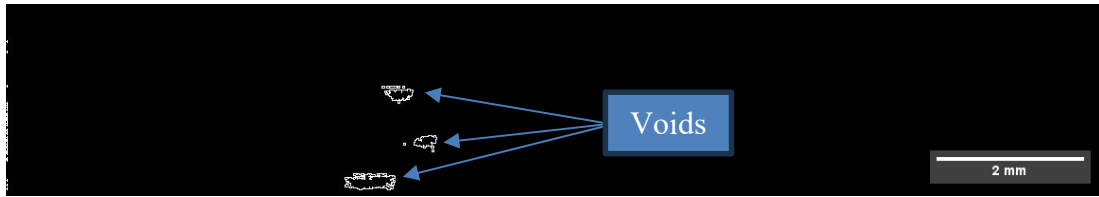


Figure 4.2: Surface of Region 2 after using ImageJ.

#### 4.1.2 Ion Polishing

The Figure 4.3 below shows the specimen after 6 hours and 10 hours of ion polished from side view of observation surface. The side of surface of 6 hours polishing can be considered as clean cut due to straight line as of polished edge as shown in the figure. However, when the ion polishing timer set to higher than 6 hours which is 10 hours, the curved edges is appeared. After carefully investigation, the shielding plate that cover the specimen became melted to the half-circle shape. That is the reason behind the curved edge that appeared after 10 hours of polishing. Due to curved edge, it affects the observation surface that need to be analysed.

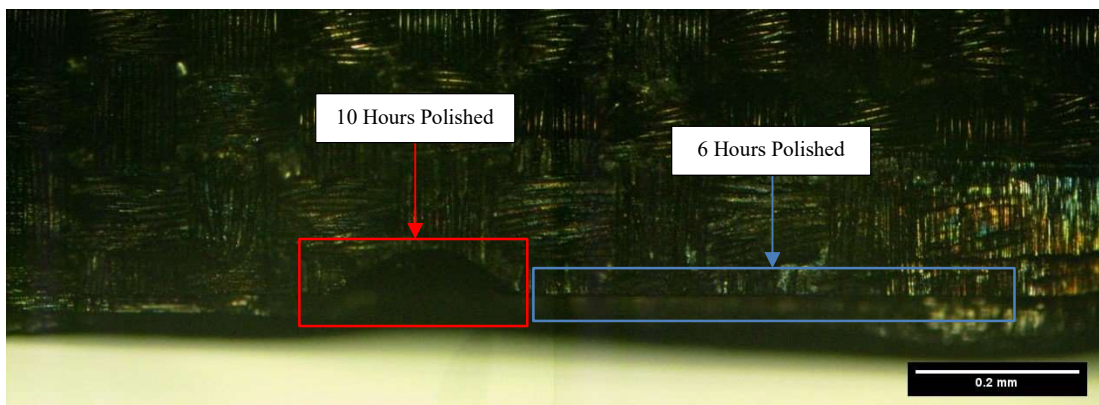


Figure 4.3: Side view from observation surface after ion polishing.

The Figure 4.4 below shows observation surface after 6 hours and 10 hours of ion polishing. After 6 hours of ion polishing, the surface became shining as mirror-like as labelled in blue rectangular in the figure. However, the curved area appears when the ion polishing timer was set to 10 hours. As discussed before, this was resulting due to melted shielding plate.

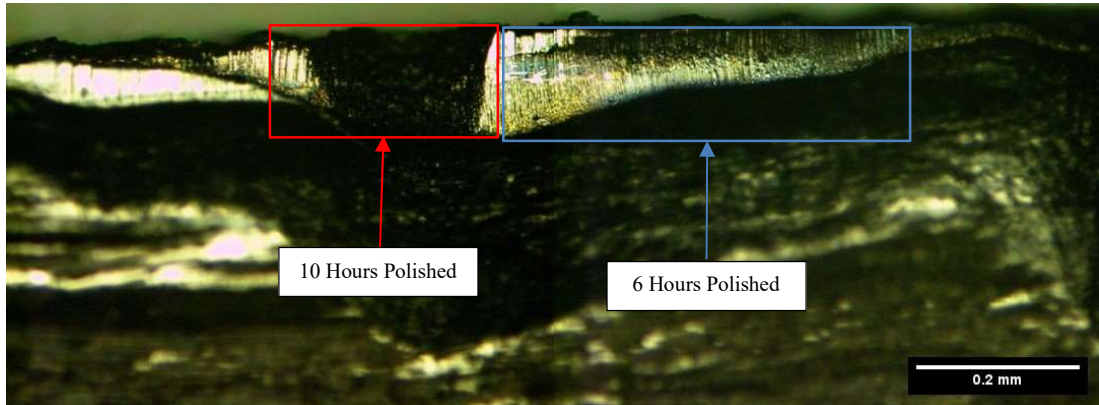


Figure 4.4: Observation surface after ion polishing.

The counter-measure was taken to obtain best surface result in ion polishing method by offsetting the shielding plate from melted surface to new surface. The same location was polished 3 times with 6 hours each session. However, the ion polishing unable to polish more than before to its limitation of depth of polishing. In result, the surface polished was same as before.

## 4.2 Void Calculation

The Table 4.1 and Figure 4.5 show the void percentage for each region with 3 depths of grinding which are 0 mm, 1 mm and 2 mm. The void percentage is calculated on void area divided by total area of the specimen. Since the specimens' size are fitted for each region, the area of each region is same which is 39 mm<sup>2</sup>.

The void percentage for each region is differ and has random patent along with depth of grinding except for Region 3 where the void percentage is decreased when the depth of grinding is increased. The void is randomly distributed along with the polymer and fibre. The value of void percentage is depending on size of void and frequency of appearances on the area. If the size of void is larger and high frequency of appearances on the area, the void percentage tend to be higher. When it is come to the patent of void formation for each area, the void is formed randomly in position and size (Gao et al., 2020).

Table 4.1: Void percentage with depth of grinding for each region.

Depth of Grinding (mm)	Void Percentage per Area (%)		
	Region 1	Region 2	Region 3
0	0.206	0.307	0.599
1	0.303	0.546	0.039
2	0.249	0.158	0.014

As Figure 4.5 below, the highest void percentage at Region 3 with 0 mm depth of grinding which is 0.599%. The lowest void percentage also at Region 3 but at 2 mm depth of grinding which is 0.014%. Comparing the differences between void percentage with depth of grinding for each region, Region 3 has larger void percentage



differences between depth of grinding other than other region from 0.599% to 0.014%. Region 2 has intermediate differences which is from 0.546% to 0.158% while Region 1 has lowest differences which is from 0.303% to 0.206%.

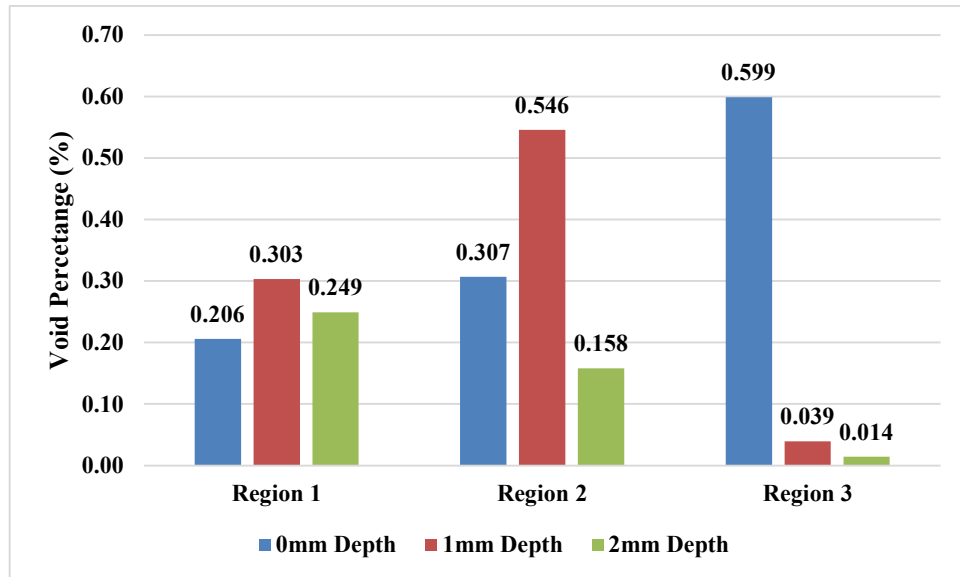


Figure 4.5: Bar chart of void percentage with depth of grinding for each region.

For average void percentage per area for each region is shown in Table 4.2 and Figure 4.6 below. The average of void percentage is calculated based on summing values of void percentage within the depth of grinding and divided by number of depths of grinding which is 3. The Region 2 has highest average void percentage while Region 3 has the lowest average. This statement shows that Region 2 has more void formation other than Region 1 and 3.

Table 4.2: Average void percentage per area for each region.

Region	Average Void Percentage per Area (%)	Standard Deviation
1	0.253	0.049
2	0.337	0.149
3	0.217	0.331

Based on Figure 4.6 below, the solid line shows the trend of average void percentage along with regions. As stated before, the void formation may be differed for each region. However, the solid line provided information according to range of void formation that might be appeared in the CFRP which is from 0.217% to 0.337%.

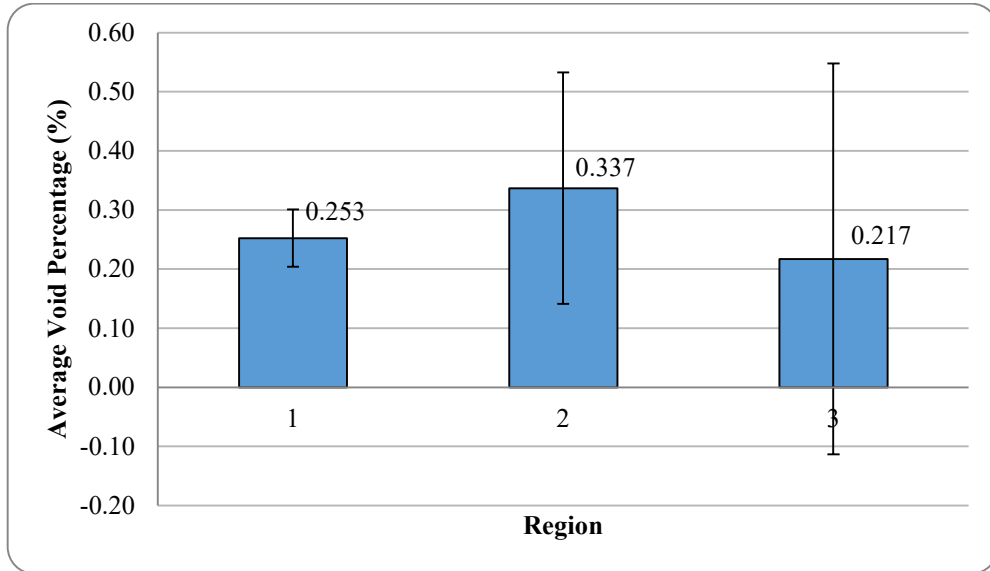


Figure 4.6: Bar graph of average void percentage per area against 3 regions.

### 4.3 Mechanical Properties

#### 4.3.1 Tensile Stress

The Table 4.3 below shows the experimental result for tensile testing. The result is compared with the average void percentage along with its maximum tensile stress and tensile extension when the specimens were broken due to applied load. At Region 3, the average void is lowest than Region 1 and 2. Due to low of void percentage, the maximum tensile stress is highest among the other region. In contrast, Region 2 consist of highest average void. In result, the maximum tensile stress obtained from Region 2 is lowest among the other region. Relating to values of maximum tensile stress, the specimen with lower maximum tensile stress tend to break at lower tensile extension.

Table 4.3: Experimental result for tensile testing.

<b>Region</b>	<b>Average Void Percentage per Area (%)</b>	<b>Maximum Tensile Stress (MPa)</b>	<b>Tensile Extension at Break (mm)</b>
<b>1</b>	0.253	907.287	6.642
<b>2</b>	0.337	846.146	6.012
<b>3</b>	0.217	914.517	6.694

The relation between average void percentage and maximum tensile stress can be seen in Figure 4.7 below. The solid line shows the values of plotted maximum tensile stress with average void percentage while the dotted line shows the trendline of the plotted graph. According to the trendline, the values of maximum tensile stress is decreased when the average void percentage is increased. From this result, it can be concluded that the maximum tensile stress is negative proportional to the average void

percentage. The claim were made that highest strength was the one with the lowest fraction of voids, showing the increment of void contents was a factor in the decrease in strength of CRFP (Hall *et al.*, 2022).

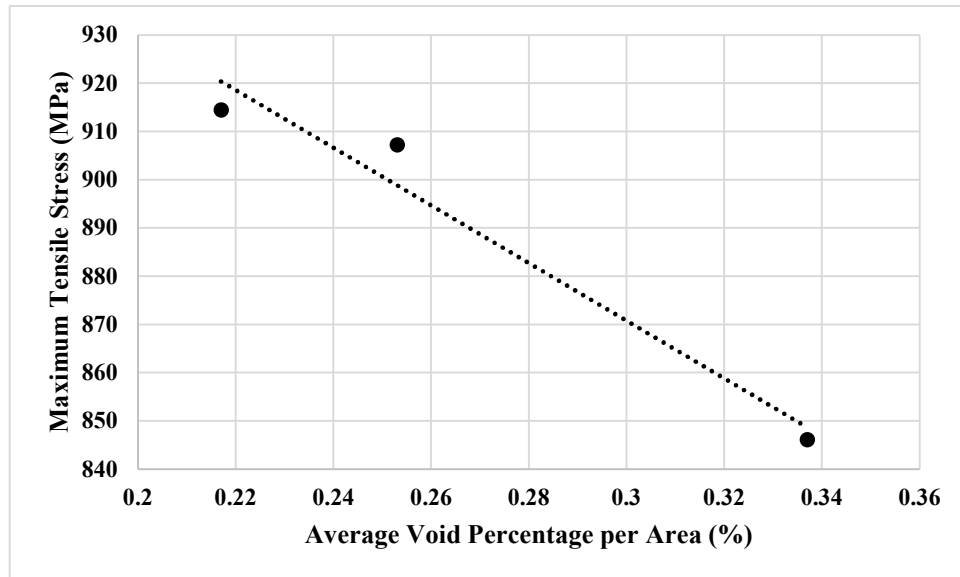


Figure 4.7: Graph of maximum tensile stress against average void.

### 4.3.2 Flexural Stress

The Table 4.4 below shows the experimental result for the flexural test. The result is compared between average void percentage and maximum flexural stress along with its extension when the specimen was broken. Since the Region 3 has the lowest value of void percentage, its maximum flexural stress is highest among other region which is 2004.375 MPa. It can be compared to the highest value of average void which is Region 2. Region 2 consists of lower maximum flexural stress which is 1857.468 MPa due to higher average void. When it comes to flexural extension at break point, the result is a bit differ where Region 2 has a longer extension which 12.277 mm than Region 1 which is 12.033 mm even though the maximum flexural stress of Region 1 is higher than Region 2.

Table 4.4: Experimental result for flexural testing.

<b>Region</b>	<b>Average Void Percentage per Area (%)</b>	<b>Maximum Flexural Stress (MPa)</b>	<b>Flexural Extension at Break (mm)</b>
<b>1</b>	0.253	1963.608	12.033
<b>2</b>	0.337	1857.468	12.277
<b>3</b>	0.217	2004.375	12.744

The relation between average void and maximum flexural stress is showed in Figure 4.8. The solid line shows the values of plotted maximum flexural stress with average void percentage while the barely seen dotted line shows the trendline of the plotted graph. According to the trendline, the values of maximum flexural stress is decreased when the average void percentage is increased. From this result, it can be concluded that the maximum flexural stress is negative proportional to the average void percentage. As per claim, the flexural properties significantly reduced with only a small amount of void content increased (Jiang *et al.*, 2019).

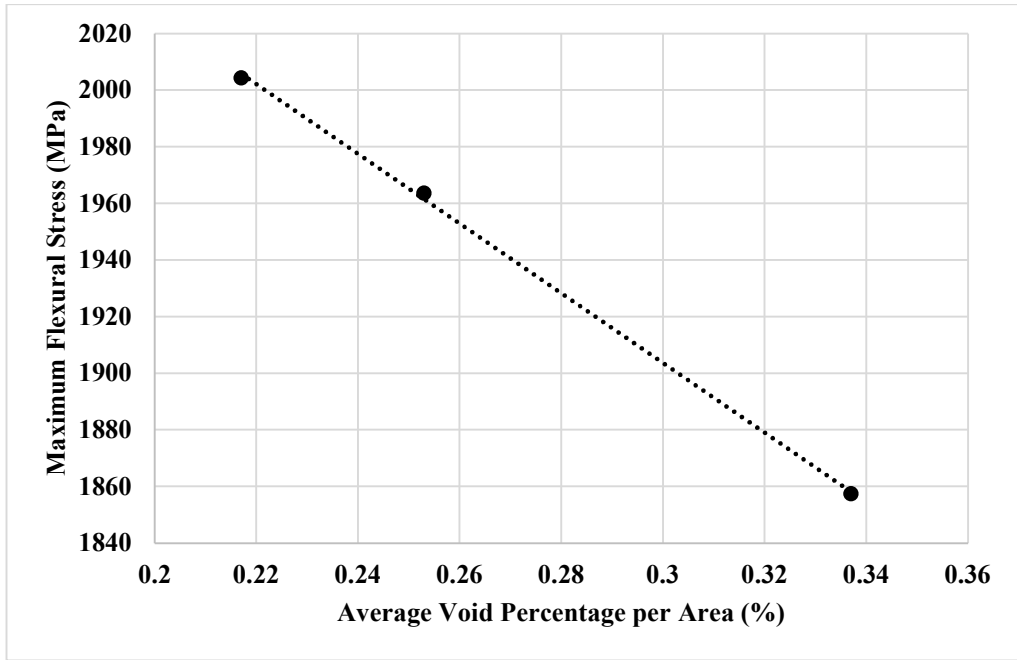


Figure 4.8: Graph of maximum flexural stress against average void.

## CHAPTER 5

### CONCLUSION AND RECOMMENDATIONS

#### 5.1 Conclusion

The specimens of Carbon Fibre Reinforced Polymer (CRFP) thermosetting composite undergo surface treatment between metallographic grinding and ion polishing has different finishing. The ion polishing method able to obtained more mirror-like finishing which is less scratches than metallographic grinding.

The second goal is achieved by comparing the average void percentage among the regions selected. The Region 2 consists of higher void formation which is 0.337% of surface area that led to reduction of mechanical properties when comparing to results of tensile and flexural testing. By comparing the average void percentage with mechanical properties, the third goal is achieved. Region 2 has lower value of maximum tensile stress which is 846.146 MPa and maximum flexural stress which is 1857.468 MPa due to high of void formation. However, small void formation does not significantly affect the mechanical properties based on small differences between mechanical properties results obtained from 3 regions.

## **5.2 Recommendation for Future Work**

Based on results obtained for surface treatment, the further study related to ion polishing method is needed to obtain the fully polished surface. The ion polishing method has variable settings including the voltage and amount of argon supplied. This setting may affect the surface finish and amount of the grinding depth.

Instead of using microscopic imaging to capture an image, X-ray computed tomography can be used to determine void formation. However, comparing the amount of void content with its mechanical properties can be done more precisely by analysing void content within specimens before undergoing mechanical testing by using non-destructive testing.



## REFERENCES

- Abdelal, N. and Donaldson, S.L. (2018) 'Comparison of methods for the characterization of voids in glass fiber composites', *Journal of Composite Materials*, 52(4), pp. 487–501. Available at: <https://doi.org/10.1177/0021998317710083>.
- Baran, I. *et al.* (2017) 'A Review on the Mechanical Modeling of Composite Manufacturing Processes', *Archives of Computational Methods in Engineering*, 24(2), pp. 365–395. Available at: <https://doi.org/10.1007/s11831-016-9167-2>.
- Fu, Y. and Yao, X. (2022) 'A review on manufacturing defects and their detection of fiber reinforced resin matrix composites', *Composites Part C: Open Access*, 8. Available at: <https://doi.org/10.1016/j.jcomc.2022.100276>.
- Gao, X. *et al.* (2020) 'Prediction of mechanical properties on 3D braided composites with void defects', *Composites Part B: Engineering*, 197. Available at: <https://doi.org/10.1016/j.compositesb.2020.108164>.
- Hall, S.E. *et al.* (2022) 'Mechanical Properties of High-Temperature Fiber-Reinforced Thermoset Composites with Plain Weave and Unidirectional Carbon Fiber Fillers', *Journal of Composites Science*, 6(7). Available at: <https://doi.org/10.3390/jcs6070213>.
- Hassan, M.S. *et al.* (2022) 'Selective Laser Sintering of High-Temperature Thermoset Polymer', *Journal of Composites Science*, 6(2). Available at: <https://doi.org/10.3390/jcs6020041>.
- Helmus, R. *et al.* (2017) 'An experimental technique to characterize interply void formation in unidirectional prepregs', *Journal of Composite Materials*, 51(5), pp. 579–591. Available at: <https://doi.org/10.1177/0021998316650273>.
- Hudson, T.B. *et al.* (2017) 'Imaging of local porosity/voids using a fully non-contact air-coupled transducer and laser Doppler vibrometer system', *Structural Health Monitoring*, 16(2), pp. 164–173. Available at: <https://doi.org/10.1177/1475921716668843>.
- Jiang, W. *et al.* (2019) 'Voids formation and their effects on mechanical properties in thermoformed carbon fiber fabric-reinforced composites', *Polymer Composites*, 40(S2), pp. E1094–E1102. Available at: <https://doi.org/10.1002/pc.24876>.
- Mehdikhani, M. *et al.* (2019) 'Voids in fiber-reinforced polymer composites: A review on their formation, characteristics, and effects on mechanical performance', *Journal of Composite Materials*. SAGE Publications Ltd, pp. 1579–1669. Available at: <https://doi.org/10.1177/0021998318772152>.

Na, W., Kwon, D. and Yu, W.R. (2018) ‘X-ray computed tomography observation of multiple fiber fracture in unidirectional CFRP under tensile loading’, *Composite Structures*, 188, pp. 39–47. Available at: <https://doi.org/10.1016/j.compstruct.2017.12.069>.

Opelt, C. V., Cândido, G.M. and Rezende, M.C. (2018) ‘Fractographic study of damage mechanisms in fiber reinforced polymer composites submitted to uniaxial compression’, *Engineering Failure Analysis*, 92, pp. 520–527. Available at: <https://doi.org/10.1016/j.engfailanal.2018.06.009>.

Saenz-Castillo, D. *et al.* (2019) ‘Effect of processing parameters and void content on mechanical properties and NDI of thermoplastic composites’, *Composites Part A: Applied Science and Manufacturing*, 121, pp. 308–320. Available at: <https://doi.org/10.1016/j.compositesa.2019.03.035>.

U, S.A., Remanan, M. and Jayanarayanan, K. (2020) *ScienceDirect Comparison of Properties of Carbon Fiber Reinforced Thermoplastic and Thermosetting Composites for Aerospace Applications, / Materials Today: Proceedings*. Available at: [www.sciencedirect.com](http://www.sciencedirect.com).

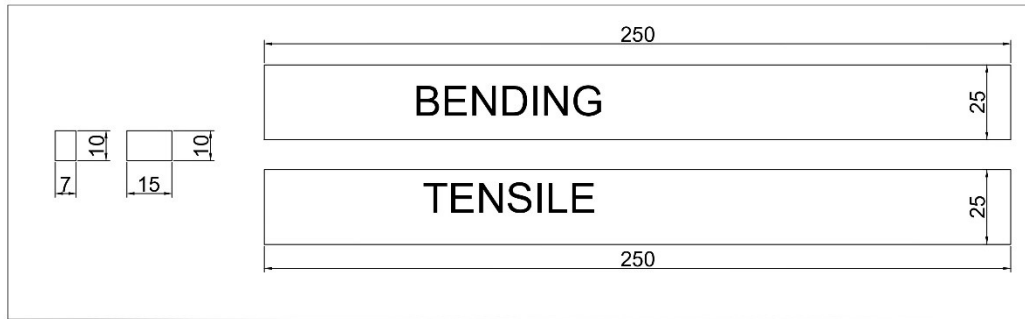
Wang, Y. *et al.* (2020) ‘Effects of surface properties of titanium alloys modified by grinding, sandblasting and acidizing and nanosecond laser on cell proliferation and cytoskeleton’, *Applied Surface Science*, 501. Available at: <https://doi.org/10.1016/j.apsusc.2019.144279>.

Xia, Z. *et al.* (2020) ‘Advances in polishing of optical freeform surfaces: A review’, *Journal of Materials Processing Technology*. Elsevier Ltd. Available at: <https://doi.org/10.1016/j.jmatprotec.2020.116828>.

Zhang, D., Heider, D. and Gillespie, J.W. (2017) ‘Determination of void statistics and statistical representative volume elements in carbon fiber-reinforced thermoplastic prepregs’, *Journal of Thermoplastic Composite Materials*, 30(8), pp. 1103–1119. Available at: <https://doi.org/10.1177/0892705715618002>.

## APPENDIX A

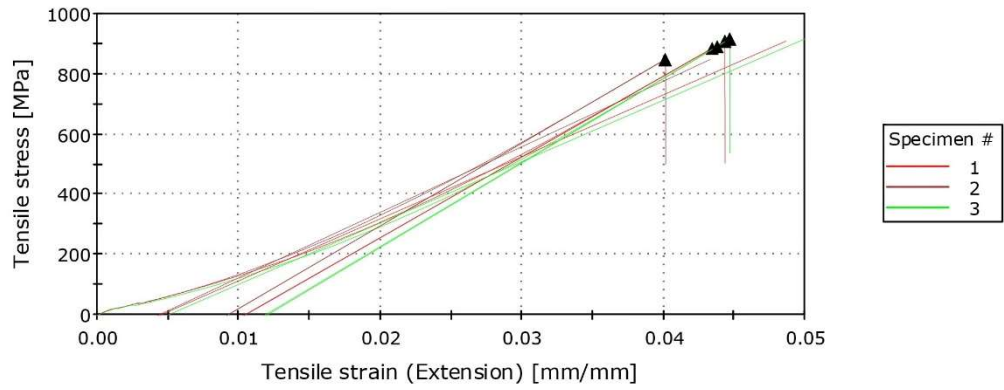
### DETAILED CUTTING PLAN FOR SPECIMENS



## APPENDIX B

### EXPERIMENTAL DATA FOR TENSILE

#### CFRP (2.6mm thk) - Tensile Testing



	Modulus (E-modulus) [MPa]	Modulus (Automatic) [MPa]	Modulus (Automatic Young's) [MPa]	Maximum Load [kN]
1	20545.452	26732.647	26781.064	58.974
2	21722.658	27352.417	27395.671	54.999
3	20324.814	27865.096	28006.656	59.444

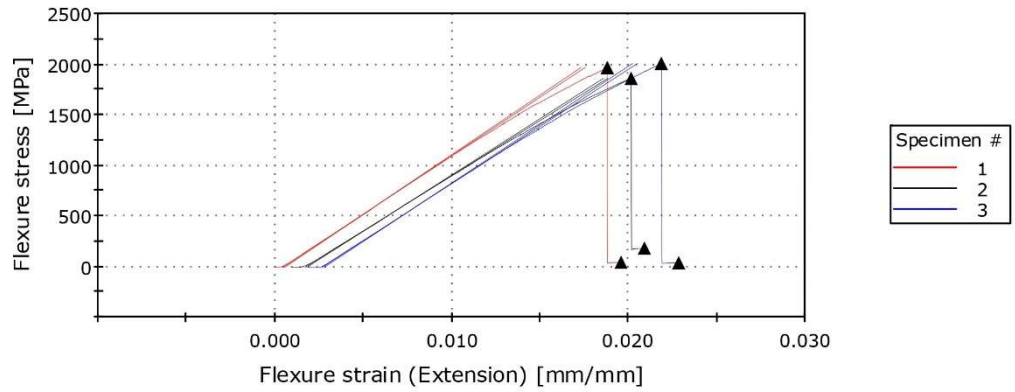
	Tensile stress at Maximum Load [MPa]	Tensile strain (Extension) at Maximum Load [mm/mm]	Tensile extension at Maximum Load [mm]	Load at Break (Standard) [kN]
1	907.287	0.044	6.642	58.974
2	846.146	0.040	6.012	54.999
3	914.517	0.045	6.694	59.444

	Tensile stress at Break (Standard) [MPa]	Tensile extension at Break (Standard) [mm]	Tensile strain (Extension) at Break (Standard) [mm/mm]
1	907.287	6.642	0.044
2	846.146	6.012	0.040
3	914.517	6.694	0.045

## APPENDIX C

### EXPERIMENTAL DATA FOR BENDING

#### CFRP (2.6mm thk) - Bending Testing



	Maximum Flexure stress [MPa]	Load at Maximum Flexure stress [N]	Flexure strain (Extension) at Maximum Flexure stress [mm/mm]	Flexure extension at Maximum Flexure stress [mm]
1	1963.608	1327.399	0.019	12.033
2	1857.468	1255.648	0.019	12.277
3	2004.375	1354.958	0.020	12.744

	Flexure stress at Break (Standard) [MPa]	Load at Break (Standard) [N]	Flexure strain (Extension) at Break (Standard) [mm/mm]	Flexure extension at Break (Standard) [mm]
1	48.412	32.726	0.020	12.534
2	187.317	126.626	0.020	12.764
3	44.465	30.058	0.021	13.373

	Modulus (Automatic) [MPa]	Modulus (E-modulus) [MPa]
1	117586.793	115197.798
2	111005.924	108728.482
3	115169.551	112631.674

**BORANG PENGESAHAN STATUS LAPORAN**  
**PROJEK SARJANA MUDA II**

Tajuk Projek : THE EFFECT OF SURFACE TREATMENT ON THE VOID CALCULATION OF THERMOSET COMPOSITE BY USING IMAGE ANALYSIS

Sesi Pengajian : SESI 2023/2024

Saya AHMAD ZULHILMI BIN AHAMAD PAUZI... mengaku membenarkan laporan Projek Sarjana Muda ini disimpan di Perpustakaan Laman Hikmah dengan syarat-syarat kegunaan seperti berikut:

1. Laporan adalah hakmilik Universiti Teknikal Malaysia Melaka.
2. Perpustakaan dibenarkan membuat salinan untuk tujuan pengajian sahaja.
3. Perpustakaan dibenarkan membuat salinan laporan ini sebagai bahan pertukaran antara institusi pengajian tinggi.
4. Sila tandakan (✓):

**SULIT\***

(Mengandungi maklumat yang berdarjah keselamatan atau kepentingan Malaysia seperti yang termaktub di dalam AKTA RAHSIA RASMI 1972).

**TERHAD\***

(Mengandungi maklumat terhad yang telah ditentukan oleh organisasi/badan di mana penyelidikan dijalankan)

**TIDAK TERHAD**

Disahkan oleh:



(TANDATANGAN PENULIS)



**DR. MIZAH BINTI RAMLI**  
Pensyarah Kanan  
Fakulti Teknologi Dan Kejuruteraan Mekanikal  
Universiti Teknikal Malaysia Melaka (UTeM)

(COP DAN TANDATANGAN PENYELIA)

Alamat Tetap: LOT 13596, JLN PARIT TALI AIR, BALAI MARAS, BATU RAKIT.  
21020 KUALA NERUS, TERENGGANU.

Tarikh: 30/1/2024

Tarikh: 30/1/2024

\*CATATAN: Jika laporan ini SULIT atau TERHAD, sila lampirkan surat daripada pihak berkuasa/organisasi berkenaan dengan menyatakan sekali tempoh laporan ini perlu dikelaskan sebagai SULIT atau TERHAD.